Published in final edited form as:
J Immunol. 2014 May 15; 192(10): 4571–4580. doi:10.4049/jimmunol.1400007.

Identification of Multiple Public T Cell Receptor Repertoires in Chronic Beryllium Disease[1]

Natalie A. Bowerman[*], **Michael T. Falta**[*], **Douglas G. Mack**[*], **Fabian Wehrmann**[*], **Frances Crawford**[†,‡], **Margaret M. Mroz**[§], **Lisa A. Maier**[*,§], **John W. Kappler**[†,‡], and **Andrew P. Fontenot**[*,†,2]

[*]Department of Medicine, University of Colorado Anschutz Medical Campus, Aurora, CO 80045, USA

[†]Integrated Department of Immunology, National Jewish Health, Denver, CO 80206, USA

[‡]Howard Hughes Medical Institute and National Jewish Health, Denver, CO 80206, USA

[§]Department of Medicine, National Jewish Health, Denver, CO 80206, USA

Abstract

Chronic beryllium disease (CBD) is a granulomatous lung disease characterized by the accumulation of beryllium (Be)-specific $CD4^+$ T cells in bronchoalveolar lavage (BAL). These expanded $CD4^+$ T cells are composed of oligoclonal T cell subsets, suggesting their recruitment to the lung in response to conventional antigen. In the present study, we noted that all BAL-derived T cell lines from HLA-DP2-expressing CBD patients contained an expansion of Be-responsive $V\beta5.1^+$ $CD4^+$ T cells. Using Be-loaded HLA-DP2-peptide tetramers, the majority of tetramer-binding T cells also expressed Vβ5.1with a highly conserved CDR3β motif. Interestingly, Be-specific, Vβ5.1-expressing $CD4^+$ T cells displayed differential HLA-DP2-peptide tetramer staining intensity, and sequence analysis of the distinct tetramer-binding subsets showed that the two populations differed by a single, conserved amino acid in the CDR3β motif. TCR Vα chain analysis of purified $V\beta5.1^+$ $CD4^+$ T cells based on differential tetramer-binding intensity showed differing TCR Vα chain pairing requirements, with the high affinity population having promiscuous Vα chain pairing and the low affinity subset requiring restricted Vα chain usage. Importantly, disease severity, as measured by loss of lung function, was inversely correlated with the frequency of tetramer-binding $CD4^+$ T cells in the lung. Our findings suggest the presence of a dominant Be-specific, Vβ5.1-expressing public T cell repertoire in the lungs of HLA-DP2-expressing CBD patients using promiscuous Vα chain pairing to recognize an identical HLA-DP2-peptide/Be complex. Importantly, the inverse relationship between expansion of $CD4^+$ T cells expressing these public TCRs and disease severity suggests a pathogenic role for these T cells in CBD.

[1]This work is supported by the following NIH grants: HL62410, HL92997, and ES011810 (to APF), HL007085 (NAB) and the Clinical & Translational Sciences Institute (UL1 TR000154) from the National Center for Advancing Translational Sciences.

[2]Address correspondence and reprint request to Dr. Andrew Fontenot, Division of Clinical Immunology (B164), University of Colorado Denver, 12700 East 19th Avenue, Aurora, CO 80045; Phone (303) 724-7192; Fax (303) 724-7295; andrew.fontenot@ucdenver.edu..

[3]Non-standard abbreviations used: beryllium, Be; Be sulfate, $BeSO_4$; bronchoalveolar lavage, BAL; chronic beryllium disease, CBD.

Keywords

Human; T cells; MHC; Lung; T cell receptors

Introduction

The antigen-specific T cell repertoire is shaped by binding of the TCR hypervariable region to a diverse array of short processed peptides bound to MHC molecules. To ensure an adequate immune response to a vast number of potential antigens, the total theoretical T cell repertoire is extremely diverse and estimated at 2.5×10^7 T cells in an individual at any given time (1-5). Hence, it is surprising that nearly identical antigen-specific or public T cells have been identified in multiple individuals (1, 3, 6). Public T cells are characterized by the expression of identical TCR Vα and/or Vβ genes that are present in the majority of subjects and dominate the response to a specific epitope. Private repertoires are those antigen-specific T cells bearing TCRs that are unique to an individual. Despite public repertoires being restricted in nature, they are typically dominant and dictate disease severity (7-11). Most studies of public repertoires have involved MHC class I-restricted $CD8^+$ T cells (1, 3, 6). Conversely, public repertoires have rarely been identified in the $CD4^+$ T cell subset due, in most cases, to unknown stimulatory antigens and the unavailability of optimal tools such as MHC class II-peptide tetramers.

Chronic beryllium disease (CBD) is a granulomatous lung disease that occurs in genetically-susceptible subjects exposed to Be in the workplace (12, 13). The onset of CBD is associated with the accumulation of Be-specific, Th1 cytokine-secreting $CD4^+$ T cells in the lung (14, 15). With a known antigen and access to pathogenic $CD4^+$ T cells from the lung, CBD is an important organ-specific immune-mediated disease, characterized by a $CD4^+$ T cell alveolitis and lung fibrosis. Genetic susceptibility to CBD is strongly linked to HLA-DP alleles that contain a glutamic acid at the 69^{th} position of the β-chain (βGlu69) (16-23), with the majority of $CD4^+$ T cells recognizing Be in an HLA-DP-restricted manner. Importantly, the HLA-DP molecules that mediate Be presentation match those implicated in disease susceptibility, confirming that the mechanism of HLA contribution to disease susceptibility depends on Be presentation to pathogenic $CD4^+$ T cells (24, 25). Previous characterization of a Be-responsive Vβ5.1/Vα22 TCR expressed on $CD4^+$ T cells derived from the lung of an HLA-DP2-expressing CBD patient showed that Be-specific T cells recognized antigen using an unconventional binding topology, with the majority of interactions occurring between TCR Vβ5.1 residues and the HLA-DP2 β1-chain (26). We have recently identified mimotopes and self-peptides (e.g., those derived from plexin A4) that in the presence of Be complete the αβTCR ligand for the Vβ5.1/Vα22 TCR (27). In addition to anchoring to HLA-DP2 and interacting with TCR, our findings suggested that Be-dependent peptides play a novel role in metal ion coordination (27). Using Be-loaded HLA-DP2-mimotope-2 and plexin A4 tetramers, $CD4^+$ T cells specific for these ligands were identified in the bronchoalveolar lavage (BAL) fluid of all HLA-$DP2^+$ CBD patients analyzed (27).

In the present study, we hypothesized that these peptides may be one of the immunodominant epitopes in the lung of HLA-$DP2^+$ CBD patients used to select T cells

expressing a public Vβ5.1$^+$ TCR repertoire. We show that a Be-loaded, HLA-DP2-mimotope-2 tetramer predominantly stained Vβ5.1-expressing CD4$^+$ T cells in the lung of HLA-DP2-expressing CBD patients, and sequencing of the TCR genes identified multiple oligoclonal T cell populations bearing a public Vβ5.1$^+$ TCR repertoire. This public T cell repertoire exhibits extremely limited variation in CDR3β expression and distinct Vα-chain pairing requirements. Thus, the conserved elements of the TCR CDR3β of this public T cell repertoire suggests that the generation of Be-responsive CD4$^+$ T cells specific for this potential immunodominant antigen allows promiscuous Vα chain pairing in order to maintain Be specificity. In addition, the dominance of these Vβ5.1-expressing public T cells in the immunopathogenesis of CBD is further supported by an inverse relationship between the expansion of these T cells and lung function.

Materials and Methods

Study population

Experiments performed in the current study used CD4$^+$ T cells derived from BAL of HLA-DP2-expressing CBD patients. The diagnosis of CBD was established using previously defined criteria (28, 29), including a history of Be exposure, the presence of granulomatous inflammation on lung biopsy, and a positive proliferative response of blood or BAL T cells to Be sulfate ($BeSO_4$) *in vitro*. Pulmonary function testing and exercise physiology were performed as part of the subject's clinical evaluation (30). Informed consent was obtained from these subjects, and the protocol was approved by the Human Subject Institutional Review Board at the University of Colorado Anschutz Medical Campus and National Jewish Health.

Identification of Be-responsive T cell expansions using dual intracellular cytokine and TCR Vβ staining

Beryllium-specific T cell lines were derived from BAL cells obtained from CBD patients as previously described (26). TCR Vβ expansions in Be-responsive, IFN-γ-expressing CD4$^+$ T cells were identified in these T cell lines using dual staining with mAbs specific for IFN-γ and the most prevalent human TCR Vβ chains. A minimum of 5×10^5 T cells were stimulated with 100 μM $BeSO_4$ for 6 hours in the presence of an equal number of autologous EBV-transformed lymphoblastoid cells. After 1 hour, brefeldin A (10 μg/mL) was added, and cells were incubated at 37°C in a humidified 5% CO_2 atmosphere for the remaining 5 hours. Washed cells were stained with an anti-CD4-PerCP mAb (BD Bioscience) and an FcR blocking reagent (Miltenyi Biotec) and transferred to a 96-well round bottom microtiter plate for incubation with 24 PE- and FITC-conjugated anti-TCR Vβ mAbs (IOTest Beta Mark, Beckman Coulter, Inc.). The Arden nomenclature system was used to designate TCR Vβs (31). This panel of anti-TCR Vβ mAbs covers approximately 70% of the TCR Vβ repertoire in healthy subjects. Cells were incubated for an additional 30 minutes at 4°C. Washed cells were fixed, permeabilized, and stained with anti-IFN-γ-APC mAb (Invitrogen) for 30 min at RT. The lymphocyte population was identified using forward and 90° light scatter patterns, and fluorescence intensity was analyzed using a LSRII flow cytometer (BD Biosciences). Data were analyzed using FlowJo software (Tree Star, Inc.).

Analysis of TCRBV5S1 gene expression in BAL-derived T cell lines and ex vivo BAL CD4$^+$ T cells

Beryllium-specific T cell lines and *ex vivo* BAL CD4$^+$ T cells were sorted based on dual staining with a Be-loaded HLA-DP2-mimotope-2 (FWIDLFETIG) tetramer (27) and an anti-TCR Vβ5.1 mAb. T cells were stained with 20 μg/mL of PE-labeled tetramer in medium containing an anti-human Fc blocking antibody for 2 hours at 37°C. Cells were stained with mAbs directed against CD3-Texas Red, CD4-PerCpCy5.5, and TCR-Vβ5.1-APC. A FITC-conjugated dump gate included mAbs directed against CD8, CD14, and CD19. Cells were stained for 30 minutes at 4°C, washed with 0.5% BSA-containing PBS and sorted using a FACS Aria flow cytometer (BD Immunocytometry Systems).

Sorted T cells were harvested, and RNA was isolated using a QIAGEN RNeasy kit according to the manufacturer's instructions. cDNA was prepared, and *TCRB* gene fragments were amplified using a *TCRBV5S1* primer (5′-ATACTTCAGTGAGACACAGAGAAAC-3′) and a *TCRBC* primer (5′-TTCTGATGGCTCAAACAC-3′). PCR products were purified using a DNA binding membrane spin column (QIAGEN), ligated into the pCR2.1 TOPO cloning vector (Invitrogen) and transformed into DH5α competent cells. Purified plasmid DNA was isolated from bacterial colonies containing appropriate inserts and sequenced with an M13 reverse sequencing primer.

In select experiments, single cells from a BAL-derived CD4$^+$ T cell line were sorted, and *TCRAV* and *BV* gene expression was determined using a 5′RACE and nested PCR method as previously described (32, 33). Briefly, T cells were stained with the PE-labeled HLA-DP2-mimotope-2/Be tetramer and anti-TCR Vβ5.1 mAb as described above and sorted as described above directly into a reverse transcription buffer.

Generation of T cell hybridomas expressing Be-specific TCRs

TCR genes were cloned into a Murine Stem Cell Virus (MSCV) plasmid for retroviral transduction into a murine TCR $\alpha^-\beta^-$ T cell hybridoma line that expresses human CD4 (designated 5KC-9C6), as described previously (26, 34). PCR fragments encoding the extracellular domains of the TCR α- and β-chains identified from each T cell were cloned into separate MSCV plasmids that encode an internal ribosomal entry site (IRES), GFP reporter for selection and either a murine Cα or Cβ domain. Full length chimeric *TCRA* and *TCRB* gene constructs were packaged as retrovirus by transient transfection of Phoenix 293T cells with the MSCV plasmids as described previously (26). 5KC-9C6 cells were transduced with filtered viral supernatant using a spin-infection protocol as previously described (35). Positively-staining cells were sorted as described above.

T cell hybridoma activation assays and HLA-DP2 tetramer staining

T cell hybridoma cells (1×10^5) and murine fibroblasts transfected to express HLA-DP2 ($2.5\text{-}5.0 \times 10^4$) were incubated overnight at 37°C with various concentrations of $BeSO_4$ and 500 nM mimotope-2 peptide, and IL-2 was measured in supernatants using the mouse IL-2 Ready-Set-Go ELISA kit (eBioscience) as described previously (26). Activation curves were generated by plotting percentage of maximal IL-2 release, $(A_{450\ (sample)} - A_{450\ (control)})$ /

(Max $A_{450\ (sample)}$ - $A_{450\ (control)}$) × 100, against antigen concentration. The concentration of $BeSO_4$ required for half-maximal IL-2 release, or EC_{50} value, was determined using non-linear regression (sigmoidal-fit, GraphPad Prism) of the activation curves.

In separate experiments, T cell hybridomas were stained with Be-loaded HLA-DP2-mimotope-2 (FWIDLFETIG) and Be-loaded HLA-DP2-plexin A4 (FVDDLFETIF) tetramers as previously described (27). An HLA-DP2-mimotope-2 tetramer that had not been pulsed with Be was used as an negative control staining reagent. In select experiments, a mAb specific for the mouse TCR Cβ domain (clone H57-597) was added at 1μg/mL to aggregate cell surface TCR prior to staining with the Be-loaded HLA-DP2-mimotope-2 tetramer (36).

Statistical analysis

ANOVA analysis was used to calculate the significant difference between samples tested. A P value of <0.05 is considered statistically significant. A Spearman correlation was used to compare the frequency of tetramer-binding $CD4^+$ T cells with markers of lung function.

Results

Beryllium-responsive Vβ5.1$^+$ CD4$^+$ T cell expansions in T cell lines derived from CBD patients

We have previously shown an increased frequency of Be-responsive Vβ5.1$^+$ CD4$^+$ T cells in the lung of HLA-DP2-expressing CBD patient 1332 (26). To determine if Be-responsive Vβ5.1$^+$ CD4$^+$ T cell expansions exist in other CBD patients, we stimulated BAL-derived $CD4^+$ T cell lines from two additional CBD patients with $BeSO_4$ and identified TCR Vβ expansions in the Be-responsive, IFN-γ-expressing T cell populations (Fig. 1). We focused on IFN-γ since it is the predominant cytokine expressed by Be-specific $CD4^+$ T cells (14, 15). Similar to patient 1332, $CD4^+$ T cell lines derived from BAL of patients 1056 and 1435 also expressed Vβ5.1$^+$ T cell expansions as measured by an increased frequency (10-30%) of IFN-γ-producing Vβ5.1$^+$ cells compared to non-IFN-γ producing cells (<6%) (Fig. 1). Other TCR Vβs were also expanded in the IFN-γ$^+$ CD4$^+$ T cell subsets. For example, Be-responsive expansions of $CD4^+$ T cells expressing Vβ1, Vβ2 and Vβ13.6 were seen in patients 1332, 1056, and 1435, respectively (Fig. 1). These findings demonstrate the presence of shared as well as unique Be-responsive TCR Vβ expansions in the BAL of CBD patients.

Beryllium-loaded HLA-DP2-mimotope-2 tetramer predominantly stains Vβ5.1-expressing CD4$^+$ T cells

Using a Be-loaded HLA-DP2-mimotope-2 tetramer, we have previously shown a high frequency of $CD4^+$ T cells in the BAL of all HLA-DP2-expressing CBD patients that bind to this pMHCII/Be complex (27). In order to determine whether the TCR repertoire of Be-responsive T cells specific for this ligand is restricted or diverse, we stained *ex vivo* BAL cells from four HLA-DP2$^+$ CBD patients with the HLA-DP2 tetramer and a subset of the anti-TCR Vβ mAbs used in Fig. 1 (Fig. 2). Due to the limited number of T cells in BAL fluid obtained from CBD patients, we chose a panel of anti-TCR Vβ mAbs that covers over

50% of the Be-responsive population in the BAL of most CBD patients (14, 37). As shown in Fig. 2*A* and similar to our previous study (27), all CBD patients possessed HLA-DP2 tetramer-binding $CD4^+$ T cells. Importantly, $CD4^+$ T cells expressing Vβ5.1 comprised the predominant tetramer-binding population. For example, 95%, 70%, 76% and 50% of tetramer-binding $CD4^+$ T cells expressed Vβ5.1 in patients 8133, 8845, 3812 and 1234, respectively (Fig. 2*A*). The overall frequency (mean ± SEM) of tetramer-binding $CD4^+$ T cells expressing Vβ5.1 in the four HLA-$DP2^+$ CBD patients was 73 ± 9.2%, suggesting that the predominant Vβ subset on $CD4^+$ T cells specific for this particular ligand is Vβ5.1 (Fig. 2*B*). Similar findings were also seen when using the Be-loaded HLA-DP2-plexin A4 tetramer (data not shown). None of the other Vβs analyzed in Fig. 2*B* were expressed on >2% of the tetramer-binding $CD4^+$ T cell subset (Fig. 2*B*). Using an irrelevant IA^b-$insulin_{10\text{-}23}$ tetramer (38), nonspecific tetramer staining was not observed (data not shown). Thus, with either IFN-γ expression as a measure of overall Be-responsiveness (Fig. 1) or HLA-DP2-mimotope-2 tetramer binding as a measure of epitope specificity (Fig. 2), $CD4^+$ T cells expressing Vβ5.1 are present in all HLA-$DP2^+$ CBD patients analyzed to date, suggesting that this Be-specific T cell subset is responding to an immunodominant antigen in the lung and may represent a public T cell repertoire. As a result, we initially focused on those Be-specific $CD4^+$ T cells expressing Vβ5.1.

Vβ5.1$^+$ T cells express a conserved CDR3β motif and represent a public TCR repertoire

Based on the presence of Be-specific Vβ5.1^+ T cell expansions in multiple CBD patients, we next determined if these expansions consisted of a public TCR repertoire having a conserved CDR3β motif. We were especially interested to see if the related CDR3β sequences identified in patient 1332 (26) were present in other CBD patients. To examine the repertoire of Vβ5.1-expressing T cells, a *BV5S1* primer was used to PCR-amplify cDNA generated from $CD4^+$ T cells derived from four BAL T cell lines and three *ex vivo* BAL samples from CBD patients. The PCR products from each sample were cloned, and bacterial isolates were selected and sequenced to determine the nucleotide and deduced amino acid sequences of the CDR3β. A highly related CDR3β motif was evident in all patients studied (Fig. 3). This conserved CDR3β motif consists of an identical length, conserved joining (J) region expression (*BJ2S5* or *BJ1S4*), and homologous amino acid residues surrounding an essential glutamine (Q) residue at position 97 of the β-chain (Fig. 3). For example, surrounding the Q in the NDβN of these related CDR3βs, small, noncharged amino acids such as alanine (A), glycine (G) and serine (S) were preferred (Fig. 3). Two predominant CDR3β sequences were present in all CBD patients described here, consisting of either AQGG or GQGG in the NDβN and using *BJ2S5* (Fig. 3). Figure 4 shows examples of identical or nearly identical β-chain amino acid sequences in different patients that were encoded by different nucleotides (i.e., expressed by different Vβ5.1^+ T cell clones), thus precluding the possibility of a PCR contamination or artifact. The nucleotides that comprise the predominant AQGG and GQGG populations shown in Fig. 4 are primarily encoded by germline *BV5S1* (highlighted in blue) and *BD1* (red). The complete *BV5S1* gene is expressed in these public β-chains with the last nucleotide (guanine) of the *BV5S1* gene dictating the expression of an A or G at position 1 of NDβ1N. Few N-region additions are used to generate the conserved XQGG motif in NDβ1N, with ~50% of the unique sequences having as few as 2-3 N-region nucleotide additions (black) (Fig. 4). Taken together, these findings

provide strong evidence for the selection and expansion of particular *TCRB* gene-expressing T cells in response to the same antigenic stimulus found in the lung of all HLA-DP2-expressing CBD patients.

Beryllium-loaded HLA-DP2-mimotope-2 tetramer detects distinct Vβ5.1 clonal populations of T cells

Using the Be-loaded HLA-DP2-mimotope-2 tetramer, we noted two distinct Vβ5.1$^+$ tetramer-binding populations. As shown in Fig. 5*A*, tetramer-binding Vβ5.1$^+$ CD4$^+$ T cells from T cell lines derived from CBD patients 1435 and 1056 could be divided into high and low intensity (tet^{hi} and tet^{lo}) groups based on tetramer staining. Similar to the *ex vivo* BAL cells shown in Fig. 2*A*, the Be-loaded tetramer stained predominantly Vβ5.1-expressing CD4$^+$ T cells (e.g., 82% and 86% for the T cell lines derived from CBD patients 1435 and 1056, respectively) (Fig. 5*A*). The tet^{hi} and tet^{lo} populations from patient 1435 were isolated by FACS sorting, and junctional region nucleotide sequencing of the *BV5S1* PCR products revealed subtle amino acid differences in the conserved CDR3β motif (Fig. 5*B*). Variability in the amino acid composition between the tet^{hi} and tet^{lo} populations was mainly found at position 96 of the conserved XQGG motif in the CDR3β (Fig. 5*B*). The tet^{hi} T cells predominantly expressed an A at this position, whereas tet^{lo} T cells expressed a G or S residue (Fig. 5*B*). For example, in patient 1435, the predominant AQGG motif in the CDR3β of the tet^{hi} population was observed in 86% of the sequenced bacterial clones while SQGG was expressed in 11% of clones tested (Fig. 5*B*). Both of these CDR3β chains were paired with *BJ2S5*. The CDR3βs comprising the tet^{lo} population expressed a more diverse set of amino acids with 50% of the sequences expressing SQGG, 24% MGQGG, and 15% GQGG, coupled with either *BJ2S5* or *BJ1S4* (Fig. 5*B*). Similar to patient 1435, the tet^{hi} population from patient 1056 exclusively expressed an AQGA sequence (Fig. 5*C*). The tet^{lo} population expressed a diverse set of Vβ5.1 sequences with 50% of the Vβ5.1 chains expressing SQGG and 24% GQGG. Our findings suggest that the high frequency clonotypes in the tet^{hi} and tet^{lo} sorted populations are the predominant T cell populations. Whether the low frequency *TCRBV* sequences represent a true subset or the result of cross-contamination resulting from cell sorting of closely-related populations is unknown.

Subtle differences in CDR3β composition of the Vβ5.1 chain affect Vα chain requirements and maintenance of Be specificity

Next, we queried whether differences in TCR Vα chain usage could account for differing HLA-DP2 tetramer binding affinities in highly-related Vβ5.1 chains. For the tet^{lo} Vβ5.1$^+$ T cell population, we focused on the GQGG CDR3β since it was expressed on CD4$^+$ T cells derived from the BAL of multiple CBD patients (see Fig. 4). Single cell PCR on sorted tet^{hi} and tet^{lo} Vβ5.1$^+$ T cell populations from patient 1435 was used to determine the accompanying native Vα chains. We identified Vα1 chain pairing with the tet^{hi} Vβ5.1 (AQGG) chain and Vα8 chain pairing with the varying Vβ5.1 chains isolated from the tet^{lo} population (Fig. 6). Both the Vα1$^+$ and Vα8$^+$ TCRs utilized the Jα28 gene segment that encodes an essential tyrosine (Y) at position 95 of the CDR3α (bolded in Fig. 6) (26). We have previously shown that a Be-specific, Vβ5.1/Vα22-expressing T cell hybridoma with a CDR3β containing AQGG-Jβ2.5 chain could pair with multiple Vα chains, including Vα22, Vα8 and Vα9, with the sole α-chain requirement being a Y expressed by Jα28 (26). We

sought to determine the extent of Vα chain cross-pairing for the AQGG and GQGG CDR3β Vβ5.1 chains isolated from patient 1435. These Vβ5.1 chains were paired with Vα22, Vα8, Vα9 or Vα1 (CDR sequences shown in Table S1), and the resultant TCRs were expressed on the surface of an $\alpha^{-}\beta^{-}$ murine T cell hybridoma in equivalent amounts (Fig. S1). The hybridomas were stained with PE-labeled, HLA-DP2-mimotope-2/Be and HLA-DP2-plexin A4/Be tetramers (Fig. 7*A*). Although tetramer staining intensity varied, T cell hybridomas expressing Vβ5.1 with the AQGG NDβN region stained with both tetramers when paired with all of the Vα chains tested (Fig. 7*A*). Conversely, the Vβ5.1 chain expressing the GQGG NDβN region could only bind to the Be-loaded HLA-DP2-mimotope-2 tetramer when paired with its native Vα8 chain (Fig. 7*A*), and none of the GQGG-expressing hybridomas were capable of binding to the HLA-DP2-plexin A4/Be tetramer.

To confirm the Be-specificity observed by tetramer staining, IL-2 secretion by T cell hybridomas expressing different Vβ5.1/Vα TCR pairs was measured in response to $BeSO_4$ and an optimal concentration of mimotope-2 using HLA-DP2-expressing fibroblasts as antigen-presenting cells. Similar to HLA-DP2 tetramer staining, all of the T cell hybridomas expressing Vβ5.1 with the AQGG NDβN region and paired with Vα22, Vα8, Vα9 or Vα1 secreted identical levels of IL-2 in response to antigen exposure (Fig. 7*B*). On the other hand, only the GQGG-expressing Vβ5.1 chain paired with Vα8 was Be-specific and secreted IL-2 after mimotope-2/Be exposure. Finally, the Vα8 chain was the optimal α-chain for pairing with both the AQGG- and GQGG-containing Vβ5.1 chains as indicated by a shift in the IL-2 response curve to the left and a 4-fold lower EC_{50} value (Fig. 7*C*). Thus, subtle differences in the CDR3β can significantly affect the TCR Vα chain pairing required for an optimal response to Be.

Identification of an additional Be-specific public T cell repertoire

Although our data clearly show that $V\beta5.1^{+}$ $CD4^{+}$ T cells comprise the predominant HLA-DP2 tetramer binding population, other Vβs are also capable of binding to the HLA-DP2-mimotope-2/Be tetramer (Fig. 2*A*). Approximately 50% of Be-loaded HLA-DP2 tetramer-binding T cells from patient 1234 expressed a Vβ other than Vβ5.1 (Fig. 2*A*), and the other tetramer-binding Vβ(s) was not identified with our panel of anti-TCR Vβ mAbs (Fig. 2*B*). Thus, we sorted $tetramer^{+}$ $V\beta5.1^{-}$ $CD4^{+}$ T cells, and the TCR Vα and Vβ chains utilized by these T cells were identified by PCR using a complete set of primers specific to *TCRAV* and *BV* genes. We identified *BV18S1* sequences in patients 1234 and 3812 expressing a CDR3β motif with a Q residue surrounded by smaller amino acids (Fig. 8*A*), similar to that described for Vβ5.1. For both 1234 and 3812, the accompanying TCR α-chain was *AV4S2*, with a related CDR3α and *AJ38* as shown in Fig. 8*A*. To demonstrate Be responsiveness of the Vβ18/Vα4 TCRs, we expressed each TCR on the surface of a murine T cell hybridoma and measured for IL-2 secretion after $BeSO_4$ stimulation (Fig. 8*B*). T cell hybridomas expressing Vα4 and Vβ18 chains identified in patients 1234 and 3812 were indeed Be-specific and secreted identical levels of IL-2 in the presence of mimotope-2 peptide, $BeSO_4$, and HLA-DP2-expressing antigen-presenting cells. As shown in Fig. 8*C*, both Vβ18-expressing T cell hybridomas also bound the Be-loaded HLA-DP2-mimotope-2 tetramer. Although not examined extensively, our findings of nearly identical Be-responsive Vβ18/

Vα4-expressing $CD4^+$ T cells found in the lungs of two CBD patients suggests the presence of an additional public TCR repertoire.

Loss of lung function in CBD patients correlates with increased frequency of Be-loaded HLA-DP2-mimotope-2 tetramer staining of $CD4^+$ T cells

In order to demonstrate that the public Vβ5.1-expressing T cells are pathogenic in HLA-DP2-expressing CBD patients, we assessed the relationship between frequency of $tetramer^+$ $CD4^+$ T cells in the BAL of 7 CBD patients with parameters of lung function. Decreases in lung physiologic measures, such as forced vital capacity (FVC) and forced expiratory volume in one second (FEV_1), and exercise capacity, as measured by workload, are associated with worsening lung fibrosis (30). As shown in Fig. 9, an inverse correlation ($r = -0.93$; $p = 0.007$) was seen between the percentage of $tetramer^+$ $CD4^+$ T cells in the BAL and FVC (percent predicted). Similarly, an inverse correlation was seen between the frequency of Be-responsive $CD4^+$ T cells specific for this αβTCR ligand and FEV_1 (percent predicted; $r = -0.82$; $p = 0.03$)) and work load ($r = -0.65$; $p = 0.04$) (Fig. 9). Conversely, no correlation was noted between tetramer staining and gas exchange (data not shown). Collectively, these data provide a link between the expansion of Be-specific public Vβ5.1-expressing $CD4^+$ T cells in the target organ of CBD patients and disease severity.

Discussion

Pathological immune responses to metal ions such as Be are among the most common causes of T cell-mediated hypersensitivities in humans, yet the nature of antigen presentation and subsequent T cell recognition is poorly characterized. Similar to recognition of self-peptides by autoimmune TCRs (39-43), Be-specific TCRs utilize an unconventional binding topology to recognize the HLA-DP2-peptide/Be complex (26). We have recently identified mimotopes and self-peptides that complete the αβTCR ligand for a set of Be-specific TCRs derived from the lung of a CBD patient, and Be-loaded HLA-DP2-mimotope-2 tetramers identified $CD4^+$ T cells specific for this complex in all HLA-DP2-expressing CBD patients (27). In the current study, we identify 1) an epitope-specific public TCR Vβ5.1 and Vβ18 repertoire expressed on $CD4^+$ T cells derived from the lungs of CBD patients; 2) TCR Vα chain promiscuity based on Be-loaded HLA-DP2-mimotope-2 tetramer staining affinity; and 3) a link between expansion of $CD4^+$ T cells expressing these public Vβ5.1 TCRs and disease severity, suggesting a pathogenic role for this T cell subset in CBD. Collectively, the identification of public, HLA-DP2-restricted T cell repertoires will aid in our understanding of the role of charged polymorphic amino acids (e.g., βGlu69) in HLA-DP molecules and the generation of immunodominant epitopes in driving the development and progression of CBD.

To date, most public T cell repertoire studies have focused on MHC class I-restricted $CD8^+$ T cells specific for either infectious agents or malignant cells (1, 3, 6), and soluble MHC-based tetramer technology has been used to track these antigen-specific $CD8^+$ T cell responses in human disease (44-47). Unfortunately, the use of MHC class II tetramers has lagged due to technical issues in generating the reagents, suboptimal staining procedures and low frequencies and affinities of antigen-specific $CD4^+$ T cells (36, 48, 49). To our

knowledge, this is the first study to use a soluble MHC class II-peptide tetramer to identify and characterize public, HLA-DP2-restricted $CD4^+$ T cell repertoires. Our success in detecting *ex vivo* Be-specific $CD4^+$ T cells in the BAL of CBD patients is likely related to the high affinity of these TCRs for the HLA-DP2-mimotope-2/Be complex, with a K_D of 4.6 μM as measured by surface plasmon resonance (27). This value is at the higher end for most TCR-pMHC interactions, which typically range between 10 and 100 μM (50).

Public T cell repertoires are defined by the expression of conserved V, CDR3, and J regions (6). Importantly, this type of TCR bias has been infrequently demonstrated in $CD4^+$ T cells obtained from blood or the target organ of human subjects. Here, we utilized Be-loaded HLA-DP2-mimotope-2 tetramers to identify and characterize public Vβ5.1 and Vβ18 T cell repertoires in the lung of HLA-DP2-expressing CBD patients. We showed that nearly identical $V\beta5.1^+$ $CD4^+$ T cells exist in *ex vivo* BAL T cells and long-term T cell lines derived from the lung of HLA-$DP2^+$ CBD patients. The TCR Vβ5.1 chains display TCR bias with expression of highly conserved Vβ5.1, CDR3β, and J regions. The CDR3β core motif consists of four amino acids (XQGG) at the V/D/J junction where X at position 96 of the TCR β-chain represents small, noncharged amino acids such as A, G and S. This position is encoded by germline nucleotide deletions and non-templated nucleotide insertions during V-D joining. Interestingly, the entire *TCRBV5S1* gene is encoded in the public repertoire, with the last nucleotide of this gene likely providing the first essential nucleotide (guanine) that is required to encode the A and G at position X of the XQGG motif. In addition, both the QG and GQG motifs are encoded by germline *BD1*. Thus, the combination of the maintenance of the entire *BV5S1* germline gene segment and the strict requirement for *BD1* are the preferred mechanism for the generation of the XQGG motif in this public repertoire (1, 3). Our previous site-directed mutagenesis study showed the importance of the Q since mutating it to an A abolished the Be-induced T cell response (26). On the other hand, small variations in amino acid composition are tolerated at the other positions of the motif, in particular A at positions 98 and 99.

Previous studies have shown that non-germline components of the CDR3β can influence TCR Vα and Vβ chain pairing (51, 52). Here, we showed that a Be-loaded HLA-DP2 tetramer differentially stained distinct $CD4^+$ T cell populations. These T cell subsets vary at the first position of the conserved XQGG motif of the CDR3β loop such that a single non-germline-derived methyl group dictates the extent of Vα chain cross-pairing needed to maintain antigen specificity. The $GQGG^+$ Vβ5.1 tet^{lo} chain requires pairing with the native Vα8 chain to generate a Be-specific response. For pairing with the tet^{hi} Vβ5.1 AQGG chain, the requirement for a specific Vα chain was more promiscuous, with multiple Vα chains expressing differing germline CDR1α and 2α loops being sufficient to maintain Be recognition. The only α-chain requirement was a conserved J region (Jα28) with an essential Y at position 95 of CDR3α (26). Our findings suggest that the tet^{hi} T cells are dominant and have a competitive advantage compared to the tet^{lo} T cells due to their ability to pair with multiple Vα chains, thus increasing the likelihood of their being highly represented in the repertoire.

Glycine-rich CDR3βs can generate cross-reactive TCRs due to the flexible nature of this loop (53). Increased flexibility guarantees T cell responsiveness and elimination of a wide

range of pathogens (5). We suggest that the glycine-rich GQGG$^+$ CDR3β loop from the tet^{lo} T cell population is more flexible than the tet^{hi} AQGG$^+$ CDR3β loop due to the absence of the additional methyl group. The GQGG$^+$ Vβ5.1$^+$ chain requirement for Vα8 chain pairing may involve enhanced interchain stabilization from amino acids expressed in the CDR1α and 2α, which may not be required by the more rigid AQGG$^+$ CDR3β loop (54). The ability of germline residues in the Vα chain to modify Vβ interactions with antigen has been previously reported in the murine IA^b-3K system (54). Even though the cognate Vα1 chain pairs with AQGG$^+$ Vβ5.1, Vα8 pairing provides optimal Be recognition as evidence by an enhanced T cell response. Perhaps the same CDR1α and/or 2α residues in Vα8 have a similar positive effect when paired with the AQGG$^+$ Vβ5.1 chain as occurs with the GQGG$^+$ Vβ5.1 chain. We know from our previous mutagenesis studies that the Vβ5.1 chain from patient 1332 dominates in TCR recognition of Be (26). This is also true here where the tet^{hi} Vβ5.1 T cells from patient 1435 do not require specific residues from CDR1α or 2α. Conversely, the tet^{lo} Vβ5.1 T cells are more dependent on the Vα chain for Be recognition, and this requirement for Vα8 may induce a different binding mode for maintenance of Be specificity.

Recent studies have shown that initial recombination events dictate the probability of the occurrence of a public T cell repertoire. These findings are supported by deep sequencing techniques that have identified memory T cell sequences in the naive T cell pool (55), diluting evidence suggesting that thymic selection events dominate in the generation of the memory T cell pool. Studies have suggested various mechanisms that support the role for initial gene recombination events in generating public repertoires. For example, convergent recombination suggests that public repertoires exist due to an increased probability of particular nucleotide sequences occurring in the naive T cell repertoire (1, 3, 45, 55, 56). If the amino acids comprising the CDR3β can be encoded by many nucleotide combinations, there is higher probability of their expression. P-nucleotide additions contributed by the Joining region during initial recombination events can also generate public repertoires (57). Furthermore, a CDR3β encoded exclusively by germline-derived nucleotides will exist more frequently than one with multiple nucleotide insertions (1, 3). Many of the public Vβ5.1$^+$ chains described here express as few as 2 to 3 nucleotide insertions in the CDR3β and were associated with restricted Jβ2.5 chain usage. Of the Jβ2 cluster, Jβ2.5 was the most likely to preferentially pair with Dβ1 (58), further supporting a role for biased gene recombination in the generation of this public repertoire. It is also possible that the public Vβ5.1 repertoire uses promiscuous Vα chain pairing to maintain TCR diversity in the lung of CBD patients. For example, in murine influenza A virus infection, the biased TCR Vα or Vβ chain dictates antigen specificity while the accompanying chain increases diversity to ensure recognition of a wide range of additional antigens (53, 59, 60).

Most TCRs express CDR3α and CDR3β regions of similar length in order to recognize antigen with optimal affinity (61). The distance between the conserved cysteine at position 91 of the V-region and the F of the J-region is 12 amino acids for CDR3β and 14 amino acids for CDR3α of the public T cells described here. It is likely that the requirement for a Y at position 95 of the CDR3α selects for an N region of 2 amino acids to ensure expression of loop size similar to CDR3β as well as to maintain proper positioning of this critical Y residue. In our previous study using site-directed mutagenesis of the amino acids in the

CDR3α region, changing the Y at position 95 to alanine abolished the beryllium-induced T cell response (26). The Y can be contributed to the *TCRA* gene either by nontemplated base additions or from the *TCRAJ* germline. Only two of 61 *AJ* gene segments (*AJ28* and *AJ45*) encode a Y that maintains proper positioning, and usage of *AJ28* is clearly the preferred mechanism for generation of these α-chains. Additionally, the requirement of Y at 95 may explain the stronger restriction of Jα usage compared to Vα usage.

The intensity of MHC tetramer staining has been correlated with T cell affinity and functional avidity (36, 62). An affinity threshold of 1-5 μM exists, where higher affinities no longer enhance functional avidity and tend to increase cross-reactivity with self-derived antigens (62, 63). Although the HLA-DP2-mimotope-2/Be tetramer stained tet^{hi} and tet^{lo} $Vβ5.1^{+}$ populations with varying intensities, these differences did not correspond with functional avidities as shown by Be-specific T cell hybridoma responses. We observed identical EC_{50} IL-2 secretion values when stimulating native tet^{hi} Vβ5.1 (AQGG)/Vα1 and tet^{lo} Vβ5.1 (GQGG)/Vα8 T cell hybridomas with varying Be concentrations. These findings suggest that the affinities of these two Vβ5.1 populations for HLA-DP2mimotope-2/Be are at the higher end of the affinity threshold and thus would not enhance the functional avidity (i.e., decrease the EC_{50} value) of the tet^{hi} population.

In conclusion, we used Be-loaded HLA-DP2-mimotope-2 tetramer to identify and characterize a public Vβ5.1 T cell repertoire, which varies in its Vα chain pairing requirements. Our findings suggest that the selection mechanism utilized to generate these public TCRs involves initial gene recombination of primarily germline-encoded genes to generate the Vβ-NDβ1N-Jβ chain and a requirement of a Y encoded by a restricted Jα28 to maintain the length of the Vα chain. The association between the presence of public $Vβ5.1^{+}$ $CD4^{+}$ T cells in the CBD lung and markers of disease severity further supports the pathogenic nature of this Be-specific T cell subset and suggests that quantitation of these T cells by tetramer staining may be used as a marker of disease progression in CBD patients.

Supplementary Material

Refer to Web version on PubMed Central for supplementary material.

References

1. Li H, Ye C, Ji G, Han J. Determinants of public T cell responses. Cell Res. 2012; 22:33–42. [PubMed: 22212481]
2. Casrouge A, Beaudoing E, Dalle S, Pannetier C, Kanellopoulos J, Kourilsky P. Size estimate of the alpha beta TCR repertoire of naive mouse splenocytes. J. Immunol. 2000; 164:5782–5787. [PubMed: 10820256]
3. Venturi V, Price DA, Douek DC, Davenport MP. The molecular basis for public T-cell responses? Nat. Rev. Immunol. 2008; 8:231–238. [PubMed: 18301425]
4. Arstila TP, Casrouge A, Baron V, Even J, Kanellopoulos J, Kourilsky P. A direct estimate of the human ab T cell receptor diversity. Science. 1999; 286:958–961. [PubMed: 10542151]
5. Meyer-Olson D, Shoukry NH, Brady KW, Kim H, Olson DP, Hartman K, Shintani AK, Walker CM, Kalams SA. Limited T cell receptor diversity of HCV-specific T cell responses is associated with CTL escape. J. Exp. Med. 2004; 200:307–319. [PubMed: 15289502]
6. Turner SJ, Doherty PC, McCluskey J, Rossjohn J. Structural determinants of T-cell receptor bias in immunity. Nat. Rev. Immunol. 2006; 6:883–894. [PubMed: 17110956]

7. Wang GC, Dash P, McCullers JA, Doherty PC, Thomas PG. T cell receptor alphabeta diversity inversely correlates with pathogen-specific antibody levels in human cytomegalovirus infection. Sci. Transl. Med. 2012; 4:128ra142.
8. Luo W, Su J, Zhang XB, Yang Z, Zhou MQ, Jiang ZM, Hao PP, Liu SD, Wen Q, Jin Q, Ma L. Limited T cell receptor repertoire diversity in tuberculosis patients correlates with clinical severity. PLoS One. 2012; 7:e48117. [PubMed: 23110186]
9. Frahm N, Kiepiela P, Adams S, Linde CH, Hewitt HS, Sango K, Feeney ME, Addo MM, Lichterfeld M, Lahaie MP, Pae E, Wurcel AG, Roach T, St John MA, Altfeld M, Marincola FM, Moore C, Mallal S, Carrington M, Heckerman D, Allen TM, Mullins JI, Korber BT, Goulder PJ, Walker BD, Brander C. Control of human immunodeficiency virus replication by cytotoxic T lymphocytes targeting subdominant epitopes. Nat. Immunol. 2006; 7:173–178. [PubMed: 16369537]
10. Ruckwardt TJ, Luongo C, Malloy AM, Liu J, Chen M, Collins PL, Graham BS. Responses against a subdominant $CD8^+$ T cell epitope protect against immunopathology caused by a dominant epitope. J. Immunol. 2010; 185:4673–4680. [PubMed: 20833834]
11. Billam P, Bonaparte KL, Liu J, Ruckwardt TJ, Chen M, Ryder AB, Wang R, Dash P, Thomas PG, Graham BS. T Cell receptor clonotype influences epitope hierarchy in the CD8+ T cell response to respiratory syncytial virus infection. J. Biol. Chem. 2011; 286:4829–4841. [PubMed: 21118816]
12. Dai S, Falta MT, Bowerman NA, McKee AS, Fontenot AP. T cell recognition of beryllium. Curr. Opin. Immunol. 2013; 25:775–780. [PubMed: 23978481]
13. Fontenot AP, Maier LA. Genetic susceptibility and immune-mediated destruction in beryllium-induced disease. Trends Immunol. 2005; 26:543–549. [PubMed: 16099719]
14. Fontenot AP, Canavera SJ, Gharavi L, Newman LS, Kotzin BL. Target organ localization of memory $CD4^+$ T cells in patients with chronic beryllium disease. J. Clin. Invest. 2002; 110:1473–1482. [PubMed: 12438445]
15. Tinkle SS, Kittle LA, Schumacher BA, Newman LS. Beryllium induces IL-2 and IFN-γ in berylliosis. J. Immunol. 1997; 158:518–526. [PubMed: 8977230]
16. Richeldi L, Sorrentino R, Saltini C. HLA-DPB1 glutamate 69: a genetic marker of beryllium disease. Science. 1993; 262:242–244. [PubMed: 8105536]
17. Richeldi L, Kreiss K, Mroz MM, Zhen B, Tartoni P, Saltini C. Interaction of genetic and exposure factors in the prevalence of berylliosis. Am. J. Ind. Med. 1997; 32:337–340. [PubMed: 9258386]
18. Wang Z, White PS, Petrovic M, Tatum OL, Newman LS, Maier LA, Marrone BL. Differential susceptibilities to chronic beryllium disease contributed by different Glu69 HLA-DPB1 and -DPA1 alleles. J. Immunol. 1999; 163:1647–1653. [PubMed: 10415070]
19. Rossman MD, Stubbs J, Lee CW, Argyris E, Magira E, Monos D. Human leukocyte antigen Class II amino acid epitopes: susceptibility and progression markers for beryllium hypersensitivity. Am. J Respir. Crit. Care Med. 2002; 165:788–794. [PubMed: 11897645]
20. Maier LA, McGrath DS, Sato H, Lympany P, Welsh K, Du Bois R, Silveira L, Fontenot AP, Sawyer RT, Wilcox E, Newman LS. Influence of MHC class II in susceptibility to beryllium sensitization and chronic beryllium disease. J. Immunol. 2003; 171:6910–6918. [PubMed: 14662898]
21. McCanlies EC, Ensey JS, Schuler CR, Kreiss K, Weston A. The association between HLA-DPB1Glu69 and chronic beryllium disease and beryllium sensitization. Am. J. Ind. Med. 2004; 46:95–103. [PubMed: 15273960]
22. Amicosante M, Berretta F, Rossman M, Butler RH, Rogliani P, van den Berg-Loonen E, Saltini C. Identification of HLA-DRPheβ47 as the susceptibility marker of hypersensitivity to beryllium in individuals lacking the berylliosis-associated supratypic marker HLA-DPGluβ69. Respir. Res. 2005; 6:94. [PubMed: 16098233]
23. Amicosante M, Deubner D, Saltini C. Role of the berylliosis-associated HLA-DPGlu69 supratypic variant in determining the response to beryllium in a blood T-cells beryllium-stimulated proliferation test. Sarcoidosis Vasc. Diffuse Lung Dis. 2005; 22:175–179. [PubMed: 16315779]
24. Fontenot AP, Torres M, Marshall WH, Newman LS, Kotzin BL. Beryllium presentation to $CD4^+$ T cells underlies disease susceptibility HLA-DP alleles in chronic beryllium disease. Proc. Natl. Acad. Sci. U S A. 2000; 97:12717–12722. [PubMed: 11050177]

25. Lombardi G, Germain C, Uren J, Fiorillo MT, du Bois RM, Jones-Williams W, Saltini C, Sorrentino R, Lechler R. HLA-DP allele-specific T cell responses to beryllium account for DP-associated susceptibility to chronic beryllium disease. J. Immunol. 2001; 166:3549–3555. [PubMed: 11207315]
26. Bowerman NA, Falta MT, Mack DG, Kappler JW, Fontenot AP. Mutagenesis of beryllium-specific TCRs suggests an unusual binding topology for antigen recognition. J. Immunol. 2011; 187:3694–3703. [PubMed: 21873524]
27. Falta MT, Pinilla C, Mack DG, Tinega AN, Crawford F, Giulianotti M, Santos R, Clayton GM, Wang Y, Zhang X, Maier LA, Marrack P, Kappler JW, Fontenot AP. Identification of beryllium-dependent peptides recognized by $CD4^+$ T cells in chronic beryllium disease. J. Exp. Med. 2013; 210:1403–1418. [PubMed: 23797096]
28. Rossman MD, Kern JA, Elias JA, Cullen MR, Epstein PE, Preuss OP, Markham TN, Daniele RP. Proliferative response of bronchoalveolar lymphocytes to beryllium. A test for chronic beryllium disease. Ann. Intern. Med. 1988; 108:687–693. [PubMed: 3282464]
29. Newman LS, Kreiss K, King TE Jr. Seay S, Campbell PA. Pathologic and immunologic alterations in early stages of beryllium disease. Re-examination of disease definition and natural history. Am. Rev. Respir. Dis. 1989; 139:1479–1486. [PubMed: 2729754]
30. Pappas GP, Newman LS. Early pulmonary physiologic abnormalities in beryllium disease. Am. Rev. Respir. Dis. 1993; 148:661–666. [PubMed: 8368637]
31. Arden B, Clark SP, Kabelitz D, Mak TW. Human T-cell receptor variable gene segment families. Immunogenetics. 1995; 42:455–500. [PubMed: 8550092]
32. Ozawa T, Kishi H, Muraguchi A. Amplification and analysis of cDNA generated from a single cell by 5′-RACE: application to isolation of antibody heavy and light chain variable gene sequences from single B cells. Biotechniques. 2006; 40:469–470. [PubMed: 16629394]
33. Ozawa T, Tajiri K, Kishi H, Muraguchi A. Comprehensive analysis of the functional TCR repertoire at the single-cell level. Biochem. Biophys. Res. Commun. 2008; 367:820–825. [PubMed: 18191637]
34. White J, Pullen A, Choi K, Marrack P, Kappler JW. Antigen recognition properties of mutant $V\beta3^+$ T cell receptors are consistent with an immunoglobulin-like structure for the receptor. J. Exp. Med. 1993; 177:119–125. [PubMed: 8380294]
35. Scott-Browne JP, Matsuda JL, Mallevaey T, White J, Borg NA, McCluskey J, Rossjohn J, Kappler J, Marrack P, Gapin L. Germline-encoded recognition of diverse glycolipids by natural killer T cells. Nat. Immunol. 2007; 8:1105–1113. [PubMed: 17828267]
36. Falta MT, Fontenot AP, Rosloniec EF, Crawford F, Roark CL, Bill J, Marrack P, Kappler J, Kotzin BL. Class II major histocompatibility complex-peptide tetramer staining in relation to functional avidity and T cell receptor diversity in the mouse $CD4^+$ T cell response to a rheumatoid arthritis-associated antigen. Arthritis Rheum. 2005; 52:1885–1896. [PubMed: 15934080]
37. Fontenot AP, Kotzin BL, Comment CE, Newman LS. Expansions of T-cell subsets expressing particular T cell receptor variable regions in chronic beryllium disease. Am. J. Respir. Cell Mol. Biol. 1998; 18:581–589. [PubMed: 9533947]
38. Crawford F, Stadinski B, Jin N, Michels A, Nakayama M, Pratt P, Marrack P, Eisenbarth G, Kappler JW. Specificity and detection of insulin-reactive $CD4^+$ T cells in type 1 diabetes in the nonobese diabetic (NOD) mouse. Proc. Natl. Acad. Sci. U S A. 2011; 108:16729–16734. [PubMed: 21949373]
39. Hahn M, Nicholson MJ, Pyrdol J, Wucherpfennig KW. Unconventional topology of self peptide-major histocompatibility complex binding by a human autoimmune T cell receptor. Nat. Immunol. 2005; 6:490–496. [PubMed: 15821740]
40. Kato Z, Stern JN, Nakamura HK, Kuwata K, Kondo N, Strominger JL. Positioning of autoimmune TCR-Ob.2F3 and TCR-Ob.3D1 on the MBP85-99/HLA-DR2 complex. Proc. Natl. Acad. Sci. U S A. 2008; 105:15523–15528. [PubMed: 18824684]
41. Li Y, Huang Y, Lue J, Quandt JA, Martin R, Mariuzza RA. Structure of a human autoimmune TCR bound to a myelin basic protein self-peptide and a multiple sclerosis-associated MHC class II molecule. EMBO J. 2005; 24:2968–2979. [PubMed: 16079912]

42. Sethi DK, Schubert DA, Anders AK, Heroux A, Bonsor DA, Thomas CP, Sundberg EJ, Pyrdol J, Wucherpfennig KW. A highly tilted binding mode by a self-reactive T cell receptor results in altered engagement of peptide and MHC. J. Exp. Med. 2011; 208:91–102. [PubMed: 21199956]
43. Yin Y, Li Y, Kerzic MC, Martin R, Mariuzza RA. Structure of a TCR with high affinity for self-antigen reveals basis for escape from negative selection. EMBO J. 2011; 30:1137–1148. [PubMed: 21297580]
44. Chen ZW, Li Y, Zeng X, Kuroda MJ, Schmitz JE, Shen Y, Lai X, Shen L, Letvin NL. The TCR repertoire of an immunodominant $CD8^+$ T lymphocyte population. J. Immunol. 2001; 166:4525–4533. [PubMed: 11254709]
45. Cohen GB, Islam SA, Noble MS, Lau C, Brander C, Altfeld MA, Rosenberg ES, Schmitz JE, Cameron TO, Kalams SA. Clonotype tracking of TCR repertoires during chronic virus infections. Virology. 2002; 304:474–484. [PubMed: 12504586]
46. Meyer-Olson D, Brady KW, Bartman MT, O'Sullivan KM, Simons BC, Conrad JA, Duncan CB, Lorey S, Siddique A, Draenert R, Addo M, Altfeld M, Rosenberg E, Allen TM, Walker BD, Kalams SA. Fluctuations of functionally distinct CD8+ T-cell clonotypes demonstrate flexibility of the HIV-specific TCR repertoire. Blood. 2006; 107:2373–2383. [PubMed: 16322475]
47. Clute SC, Naumov YN, Watkin LB, Aslan N, Sullivan JL, Thorley-Lawson DA, Luzuriaga K, Welsh RM, Puzone R, Celada F, Selin LK. Broad cross-reactive TCR repertoires recognizing dissimilar Epstein-Barr and influenza A virus epitopes. J. Immunol. 2010; 185:6753–6764. [PubMed: 21048112]
48. Kwok WW, Tan V, Gillette L, Littell CT, Soltis MA, LaFond RB, Yang J, James EA, DeLong JH. Frequency of epitope-specific naive $CD4^+$ T cells correlates with immunodominance in the human memory repertoire. J. Immunol. 2012; 188:2537–2544. [PubMed: 22327072]
49. Scriba TJ, Purbhoo M, Day CL, Robinson N, Fidler S, Fox J, Weber JN, Klenerman P, Sewell AK, Phillips RE. Ultrasensitive detection and phenotyping of $CD4^+$ T cells with optimized HLA class II tetramer staining. J. Immunol. 2005; 175:6334–6343. [PubMed: 16272285]
50. Stone JD, Chervin AS, Kranz DM. T-cell receptor binding affinities and kinetics: impact on T-cell activity and specificity. Immunology. 2009; 126:165–176. [PubMed: 19125887]
51. Bartok I, Holland SJ, Kessels HW, Silk JD, Alkhinji M, Dyson J. T cell receptor CDR3 loops influence αβ pairing. Mol. Immunol. 2010; 47:1613–1618. [PubMed: 20189651]
52. Richman SA, Aggen DH, Dossett ML, Donermeyer DL, Allen PM, Greenberg PD, Kranz DM. Structural features of T cell receptor variable regions that enhance domain stability and enable expression as single-chain VαVβ fragments. Mol. Immunol. 2009; 46:902–916. [PubMed: 18962897]
53. Naumov YN, Naumova EN, Yassai MB, Kota K, Welsh RM, Selin LK. Multiple glycines in TCR α-chains determine clonally diverse nature of human T cell memory to influenza A virus. J. Immunol. 2008; 181:7407–7419. [PubMed: 18981164]
54. Stadinski BD, Trenh P, Smith RL, Bautista B, Huseby PG, Li G, Stern LJ, Huseby ES. A role for differential variable gene pairing in creating T cell receptors specific for unique major histocompatibility ligands. Immunity. 2011; 35:694–704. [PubMed: 22101158]
55. Venturi V, Quigley MF, Greenaway HY, Ng PC, Ende ZS, McIntosh T, Asher TE, Almeida JR, Levy S, Price DA, Davenport MP, Douek DC. A mechanism for TCR sharing between T cell subsets and individuals revealed by pyrosequencing. J. Immunol. 2011; 186:4285–4294. [PubMed: 21383244]
56. Quigley MF, Greenaway HY, Venturi V, Lindsay R, Quinn KM, Seder RA, Douek DC, Davenport MP, Price DA. Convergent recombination shapes the clonotypic landscape of the naive T-cell repertoire. Proc. Natl. Acad. Sci. U S A. 2010; 107:19414–19419. [PubMed: 20974936]
57. Yassai M, Bosenko D, Unruh M, Zacharias G, Reed E, Demos W, Ferrante A, Gorski J. Naive T cell repertoire skewing in HLA-A2 individuals by a specialized rearrangement mechanism results in public memory clonotypes. J. Immunol. 2011; 186:2970–2977. [PubMed: 21282510]
58. Livak F, Burtrum DB, Rowen L, Schatz DG, Petrie HT. Genetic modulation of T cell receptor gene segment usage during somatic recombination. J. Exp. Med. 2000; 192:1191–1196. [PubMed: 11034609]

59. Day EB, Guillonneau C, Gras S, La Gruta NL, Vignali DA, Doherty PC, Purcell AW, Rossjohn J, Turner SJ. Structural basis for enabling T-cell receptor diversity within biased virus-specific CD8+ T-cell responses. Proc. Natl. Acad. Sci. U S A. 2011; 108:9536–9541. [PubMed: 21606376]

60. Zhong W, Dixit SB, Mallis RJ, Arthanari H, Lugovskoy AA, Beveridge DL, Wagner G, Reinherz EL. CTL recognition of a protective immunodominant influenza A virus nucleoprotein epitope utilizes a highly restricted Vβ but diverse Vα repertoire: functional and structural implications. J. Mol. Biol. 2007; 372:535–548. [PubMed: 17658550]

61. Moss PA, Bell JI. Comparative sequence analysis of the human T cell receptor TCRA and TCRB CDR3 regions. Hum. Immunol. 1996; 48:32–38. [PubMed: 8824571]

62. Schmid DA, Irving MB, Posevitz V, Hebeisen M, Posevitz-Fejfar A, Sarria JC, Gomez-Eerland R, Thome M, Schumacher TN, Romero P, Speiser DE, Zoete V, Michielin O, Rufer N. Evidence for a TCR affinity threshold delimiting maximal CD8 T cell function. J. Immunol. 2010; 184:4936–4946. [PubMed: 20351194]

63. Holler PD, Chlewicki LK, Kranz DM. TCRs with high affinity for foreign pMHC show self-reactivity. Nat. Immunol. 2003; 4:55–62. [PubMed: 12469116]

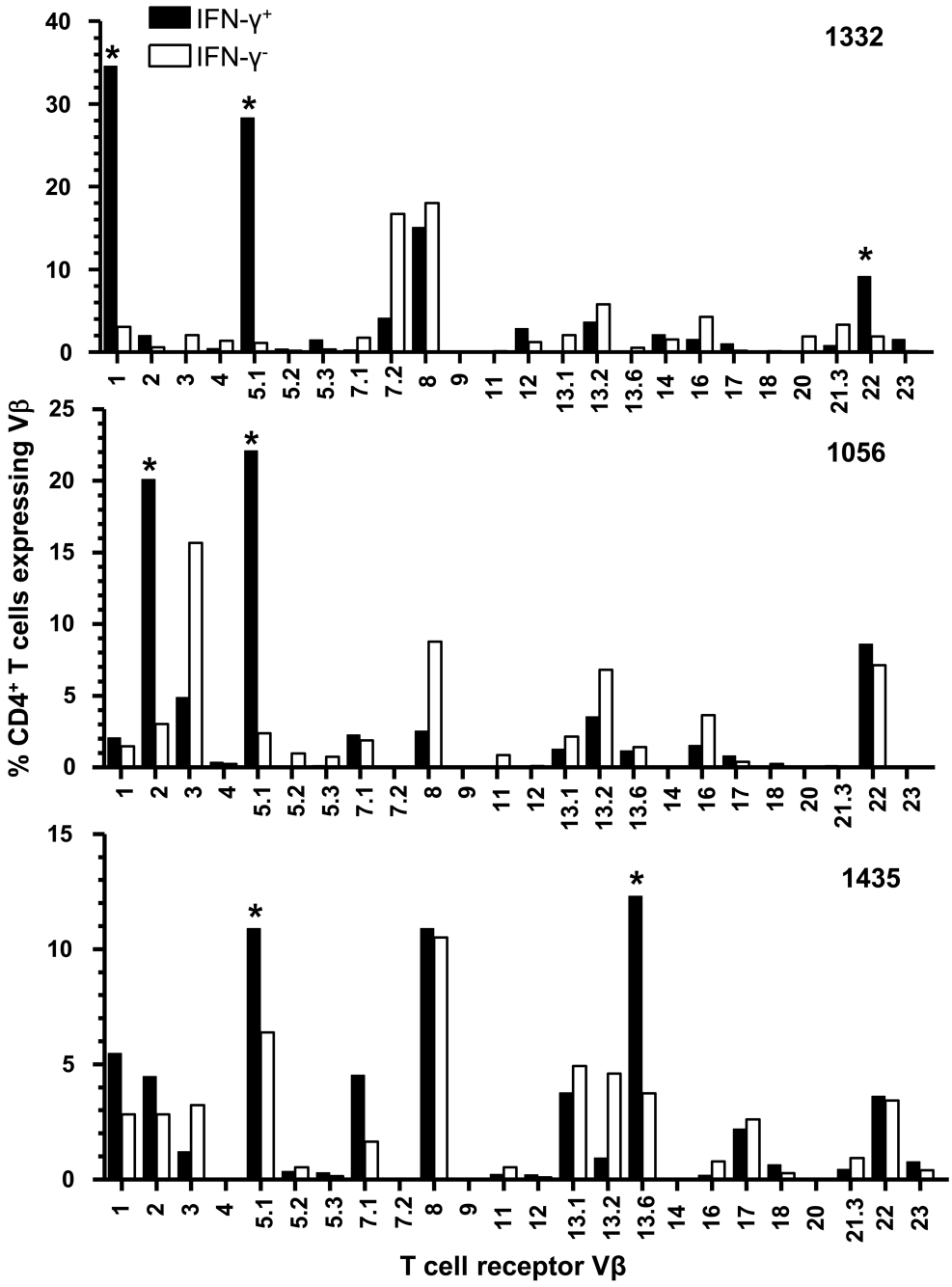

FIGURE 1.

TCR Vβ repertoire of beryllium-responsive T cells. TCR Vβ repertoire of Be-responsive, IFN-γ-expressing $CD4^+$ T cell lines derived from the bronchoalveolar lavage of HLA-DP2-expressing CBD patients. Data are expressed as the percentage of IFN-γ^+ (black bars) or IFN-γ^- (white bars) $CD4^+$ T cells expressing a particular Vβ. An *asterisk* is used to identify expanded Vβ subsets in the Be-responsive, IFN-γ-expressing $CD4^+$ T cell subset in individual patients.

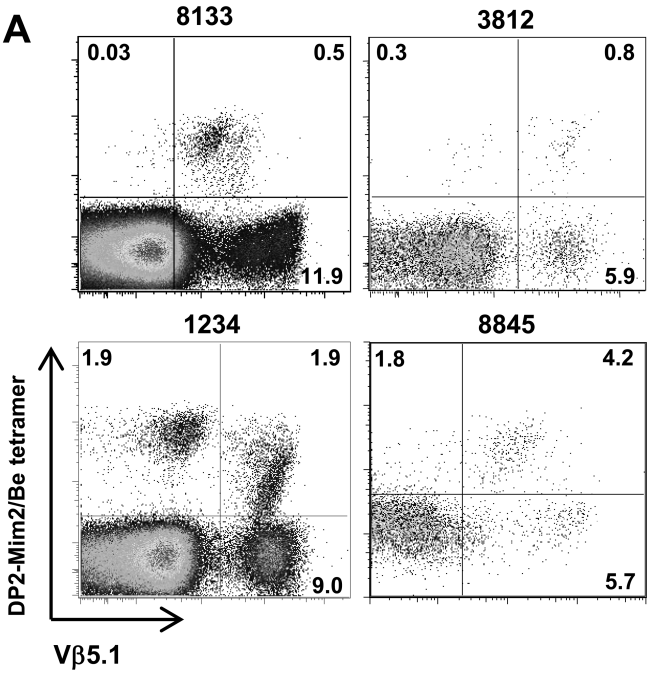

B

% tetramer+/CD4+ T cell expressing TCR Vβ

TCR Vβ	8133	8455	3812	1234
Vβ2	0	1.8	0	0.7
Vβ3	0.4	2.0	0	0.3
Vβ5.1	95	70	76	50
Vβ5.2	NT	0.83	0	NT
Vβ6.7	0.4	1.8	0	0.2
Vβ8	0	0.6	0	0.7
Vβ13.1	0.7	1.1	0	0.6
Vβ13.2	0.4	NT	NT	0.3
Vβ17	0.4	0.5	0	0.3
Vβ22	0	0.4	1.6	0.5

FIGURE 2.

HLA-DP2-mimotope 2/Be tetramer predominantly stains Vβ5.1$^+$ T cells from *ex vivo* BAL cells of CBD patients. (*A*) Representative density plots of soluble HLA-DP2-mimotope-2/Be tetramer and TCR Vβ5.1 staining of CD4$^+$ T cells from *ex vivo* BAL obtained from four HLA-DP2$^+$ CBD patients is shown. The percentage of the various staining subsets is also shown. (*B*) Summary of the frequency of tetramer staining of *ex vivo* BAL CD4$^+$ T cells from four HLA-DP2$^+$ CBD patients dually-stained with the HLA-DP2-mimotope-2/Be tetramer and a panel of anti-TCR Vβ mAbs. A box surrounding the percentage of tetramer-staining CD4$^+$ T cells that express Vβ5.1 is shown. NT, not tested.

	CDR3 Amino Acid Sequence				
Patient	Vβ5.1	NDβN	Jβ	BJ	Frequency
	91	97			
1332	C A S S L	A **Q** G G	E T Q Y F G	2.5	8/9
	C A S S L	S **Q** G G	E K L F F G	1.4	1/9
1435	C A S S L	A **Q** G G	E T Q Y F G	2.5	23/57
	C A S S	M G **Q** G G	E T Q Y F G	2.5	11/57
	C A S S L	S **Q** G G	E T Q Y F G	2.5	10/57
	C A S S L	S **Q** G G	E K L F F G	1.4	7/57
	C A S S L	G **Q** G G	E T Q Y F G	2.5	5/57
	C A S S L	A **Q** G G	E K L F F G	1.4	1/57
1056	C A S S L	A **Q** G A	E T Q Y F G	2.5	10/24
	C A S S L	S **Q** G G	E K L F F G	1.4	9/24
	C A S S L	G **Q** G G	E T Q Y F G	2.5	4/24
	C A S S L	A **Q** G G	E T Q Y F G	2.5	1/24
3421	C A S S L	A **Q** G G	E T Q Y F G	2.5	1/23
	C A S S L	G **Q** G G	E T Q Y F G	2.5	1/23
	C A S S L	S **Q** G A	E T Q Y F G	2.5	1/23
3812	C A S S L	S **Q** G G	E T Q Y F G	2.5	11/15
	C A S S L	G **Q** G G	E T Q Y F G	2.5	2/15
	C A S S L	S **Q** G G D	T Q Y F G	2.5	1/15
	C A S S L	N **Q** G G Y	I Q Y F G	2.4	1/15
8845	C A S S L	A **Q** G G	E T Q Y F G	2.5	26/36
	C A S S L	G **Q** A G	E T Q Y F G	2.5	5/36
	C A S S	Q A **Q** G G	E T Q Y F G	2.5	2/36
	C A S S L	A **Q** G A	E T Q Y F G	2.5	1/36
	C A S S L	S **Q** G G	E T Q Y F G	2.5	1/36
	C A S S L	S **Q** G G	E K L F F G	1.4	1/36
1234	C A S S L	G **Q** G G	E T Q Y F G	2.5	2/46
	C A S S L	A **Q** G G	E T Q Y F G	2.5	2/46
	C A S S L	A **Q** A G	E T Q Y F G	2.5	1/46

FIGURE 3.

Identical TCR Vβ5.1 chains identified in all HLA-DP2-expressing CBD patients. Analysis of deduced Vβ5.1 CDR3 amino acid sequences expressed on $CD4^+$ T cells derived from either *ex vivo* BAL or BAL T cell lines from a total of seven HLA-DP2-expressing CBD patients. A nearly identical CDR3β motif comprised the TCR Vβ5.1 chains was identified from either $CD4^+$ T cells sorted for HLA-DP2-mimotope-2/Be tetramer and Vβ5.1 staining (1332, 1435, 1056, 3812 and 8845) or from bulk cDNA analysis (3421 and 1234). CDR3β consists of conserved lengths, Jβ2.5/1.4 expression, and expression of a glutamine surrounded by small amino acid side chains. Glutamine at position 97 is bolded to highlight the significance of this residue in Be

recognition. The number of identical sequences (defined at the nucleotide level) is shown over the total number of sequences analyzed.

Patient	Vβ5.1					NDβ1N				Jβ2.5						Frequency
	C	A	S	S	L	**A**	Q	**G**	**G**	E	T	Q	Y	F	G	
1332	tgc	gcc	agc	agc	ttg	gcc	cag	ggg	gga	gag	acc	cag	tac	ttc	ggg	5/9
1435	-	-	-	-	-	gca	cag	ggt	gga	-	-	-	-	-	-	21/57
1056	-	-	-	-	-	gca	cag	ggg	gga	-	-	-	-	-	-	1/24
3421	-	-	-	-	-	gcc	caa	ggg	gga	-	-	-	-	-	-	1/23
1234	-	-	-	-	-	gcc	cag	gga	ggg	-	-	-	-	-	-	1/46
8845	-	-	-	-	-	gcc	cag	ggg	gga	-	-	-	-	-	-	13/36
						A	Q	G	**A**							
1056	-	-	-	-	-	gcc	cag	ggg	gca	-	-	-	-	-	-	7/24
	C	A	S	S	**L**	**A**	Q	**A**	**G**							
1234	tgc	gcc	agc	agc	ttc	gcc	cag	gcg	ggg	-	-	-	-	-	-	1/46
	C	A	S	S	L	G	Q	**G**	**G**	-	-	-	-	-	-	
1056	tgc	gcc	agc	agc	ttg	gga	cag	ggc	ggt	-	-	-	-	-	-	3/24
1435	-	-	-	-	-	gga	cag	ggg	gga	-	-	-	-	-	-	4/57
3421	-	-	-	-	-	gga	cag	ggg	ggg	-	-	-	-	-	-	1/23
3812	-	-	-	-	-	gga	cag	gga	ggt	-	-	-	-	-	-	2/15
1234	-	-	-	-	-	gga	cag	gga	ggc	-	-	-	-	-	-	1/46
						G	Q	**A**	**G**							
8845	-	-	-	-	-	ggt	cag	gcg	ggg	-	-	-	-	-	-	4/36

Vβ5.1 TGC GCC AGC AGC TTG G
Dβ1 G GGA CAG GGG GC
Jβ2.5 AC CAA GAG ACC CAG TAC TTC GGG

FIGURE 4.

Oligoclonal expansions of nearly identical *TCRBV5S1* chains expressed in multiple patients diagnosed with CBD. Shown are nucleotide and deduced amino acid sequences of two related sets of CDR3β expressing nearly identical *TCRBV5S1* chains that, in most cases, differed by a single amino acid at the first position of the NDβN region. The number of identical sequences (defined at the nucleotide level) is shown over the total number of sequences analyzed. The cysteine (C) of the β-chain is designated as position 91 with the essential glutamine (Q) at position 97. Bolded amino acids are generated by either all non-template encoded nucleotides or a combination of non-template and germline encoded nucleotides. Nucleotides highlighted in blue, red, green, and black are encoded by Vβ5.1, Dβ1, Jβ2.5, and non-template bases, respectively.

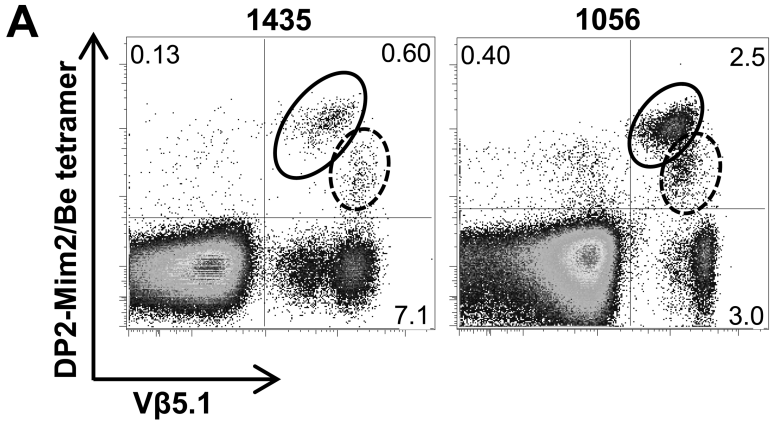

B

Cells	Vβ5.1	NDβN	Jβ	BJ	Frequency
	C A S S L	**A** Q **G G**	E T Q Y F G	2.5	29/35
	C A S S L	**A** Q G **G**	E T Q Y F G	2.5	1/35
tet^{hi}	C A S S L	**S** Q G **G**	E T Q Y F G	2.5	3/35
	C A S S L	**S** Q **G G**	E T Q Y F G	2.5	1/35
	C A S S L	**G** Q **G G**	E T Q Y F G	2.5	1/35
	C A S S **M**	G Q G **G**	E T Q Y F G	2.5	11/46
	C A S S L	**G** Q G **G**	E T Q Y F G	2.5	7/46
	C A S S L	**S** Q **G G**	E T Q Y F G	2.5	6/46
tet^{lo}	C A S S L	**S** Q **G G**	E K L F F G	1.4	15/46
	C A S S L	**S** Q **G G**	E K L F F G	1.4	1/46
	C A S S L	**S** Q G **G**	**R P M** F F G	1.4	1/46
	C A S S L	**A** Q G **G**	E K L F F G	1.4	2/46
	C A S S L	**A** Q G **A**	E T Q Y F G	2.5	3/46

C

Cells	Vβ5.1	NDβN	Jβ	BJ	Frequency
tet^{hi}	C A S S L	**A** Q G **A**	E T Q Y F G	2.5	7/7
	C A S S L	**S** Q **G G**	E K L F F G	1.4	9/17
tet^{lo}	C A S S L	G Q **G G**	E T Q Y F G	2.5	3/17
	C A S S L	G Q **G G**	E T Q Y F G	2.5	1/17
	C A S S L	**A** Q G **A**	E T Q Y F G	2.5	3/17
	C A S S L	**A** Q G **G**	E T Q Y F G	2.5	1/17

FIGURE 5.

Distinct TCR Vβ5.1 CDR3β sequences in tet^{hi} and tet^{lo} CD4^{+} T cells. (*A*) Density plots of HLA-DP2-mimotope-2/Be tetramer and TCR Vβ5.1 staining of CD4^{+} T cells from BAL-derived T cell lines of CBD patients 1435 and 1056 are shown. The tet^{hi} and tet^{lo} Vβ5.1^{+} CD4^{+} T cell subsets are enclosed in solid and dashed circles, respectively. The percentage of the various staining subsets is also shown. Deduced Vβ5.1 CDR3 amino acid sequences in the tet^{hi} and tet^{lo} CD4^{+} T cell populations of CBD patients 1435 (*B*) and 1056 (*C*) are shown. Variation between the tet^{hi} and tet^{lo} T cell populations lies in the amino acids comprising the first position of the NDβN region. The number of identical sequences (defined at the nucleotide level) is shown

over the total number of sequences analyzed. Bolded amino acids denote those that are encoded by all non-template nucleotides or a combination of non-template and germline encoded nucleotides.

Cells	TCR Vβ	Vβ	NDβN	Jβ2.5	TCR Vα	Vα	N	Jα28	Redund -ancy
tet^{hi}	5S1	CASSL	A**Q**GG	ETQY	1S5	CVV	TI	**Y**SGA	2
	5S1	CASSL	S**Q**GG	ETQY	8S1	CAA	SA	**Y**SGA	4
tet^{lo}	5S1	CASSL	G**Q**AG	ETQY	8S1	CAA	SK	**Y**SGA	2
	5S1	CASSL	G**Q**GG	ETQY	8S1	CAA	SS	**Y**SGA	1

FIGURE 6.

Deduced TCR CDR3 sequences from Vβ5.1^{+} tet^{hi} and tet^{lo} CD4^{+} T cell lines. Single cells of tet^{hi} and tet^{lo} Vβ5.1^{+} CD4^{+} T cell populations isolated from patient 1435 were sorted, and PCR was used to identify paired TCR Vα and Vβ5.1 chains. Amino acid sequences of both TCR CDR3α and CDR3β are shown for clones identified from both populations. Redundancy refers to the number of independent T cell clones that had identical *TCRA* and *TCRB* gene nucleotide sequences.

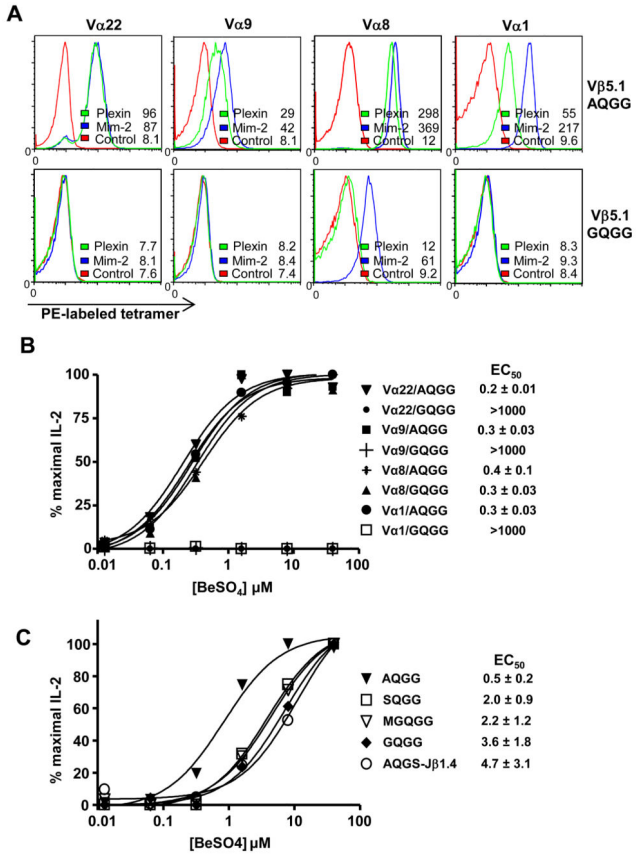

FIGURE 7.

TCR Vβ5.1 chains from $CD4^+$ T cell populations require strict Vα chain pairing to maintain Be specificity. (*A*) Hybridomas expressing $Vβ5.1^+$ AQGG or GQGG CDR3β chains were paired with multiple Vα chains on the surface of a murine T cell hybridoma and were stained with soluble Be-loaded HLA-DP2-mimotope-2 (Mim2) and HLA-DP2-plexin A4 (plexin) tetramers. An HLA-DP2-mimotope-2 tetramer without Be loading (Control) was used as a negative control. The mean fluorescence intensity (MFI) for each subset is shown. Positive tetramer staining was observed for the $AQGG^+$ Vβ5.1 chain when paired with all Vα chains tested, whereas the $GQGG^+$ chain required Vα8. With the exception of the $Vβ5.1^+$ AQGG/$Vα22^+$ T cell hybridoma, the plexin A4 tetramer stained all hybridomas with lower intensity compared to the mimotope-2 tetramer. (*B*) The hybridomas from (*A*) were stimulated overnight with 500 nM mimotope-2 peptide, varying $BeSO_4$ concentrations and HLA-DP2-transfected fibroblasts as antigen-presenting cells. Data are plotted as % maximal IL-2 secretion against concentration of Be and are representative of three independent experiments. The mean ± SEM EC_{50} values for each of the hybridomas are shown. (*C*) Stimulation of T cell hybridomas expressing a $Vα8^+$ CDR3α-CAASSYSGA$^+$ chain with varying Vβ5.1 chains isolated from the tet^{hi} and tet^{lo} T cell populations. T cell hybridomas were stimulated as in (*B*). Data are plotted as % maximal IL-2 secretion against concentration of Be and are representative of three independent experiments. The mean ± SEM EC_{50} values for each of the hybridomas are shown.

A

CBD patient	TCR Vβ18	NDβN	Jβ2.7	TCR Vα4S2	N	Jα38
1234	CASSP	**NGQAH**	EQYFG	CIVRV	WD	AGNN
3812	CASS	**PTGQAH**	EQYFG	CIVR	AY	NAGNN

B

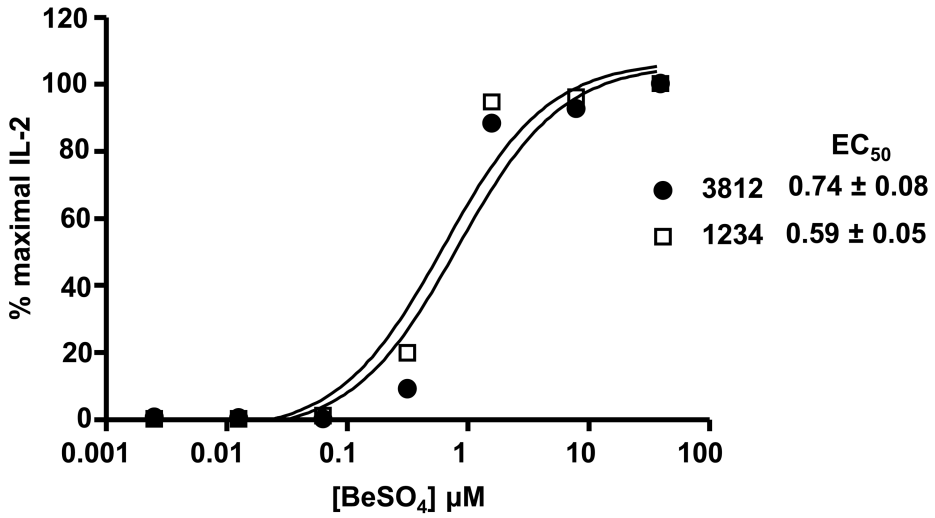

C

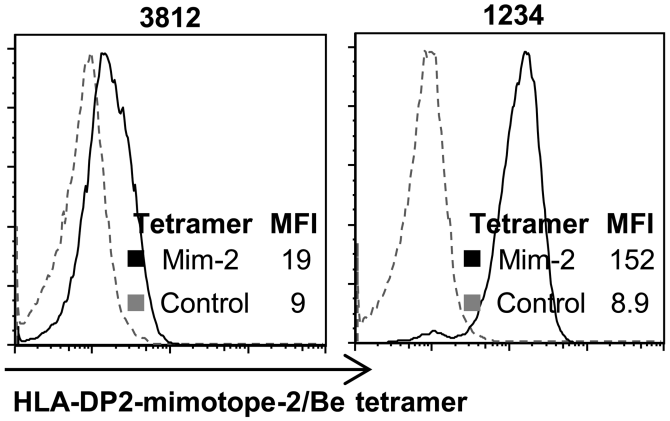

FIGURE 8.

A public Vβ18$^+$ TCR repertoire in multiple CBD patients expresses a nearly identical CDR3β motif. (*A*) Shown are the amino acid sequences of the paired Vβ18 CDR3β and Vα4 CDR3α derived from CD4$^+$ T cells from CBD patients 1234 and 3812 that bind the HLA-DP2-mimotope-2/Be tetramer. (*B*) Murine T cell hybridomas expressing the Vβ18/Vα4 TCR are Be-specific and secrete IL-2 in the presence of HLA-DP2-expressing fibroblasts, mimotope-2 peptide, and varying concentrations of $BeSO_4$. Data are plotted as % maximal IL-2 secretion against concentration of Be and are representative of three independent experiments. The mean ± SEM EC_{50} values for both hybridomas in response to Be are shown. (*C*) T cell hybridomas expressing the Vβ18/Vα4 TCRs derived from CBD patients 3812 and 1234 bind to the Be-loaded HLA-DP2-mimotope-2 tetramer (black

line). Unstained hybridoma cells were used as a negative control (dashed line). The mean fluorescence intensity (MFI) for each subset is shown.

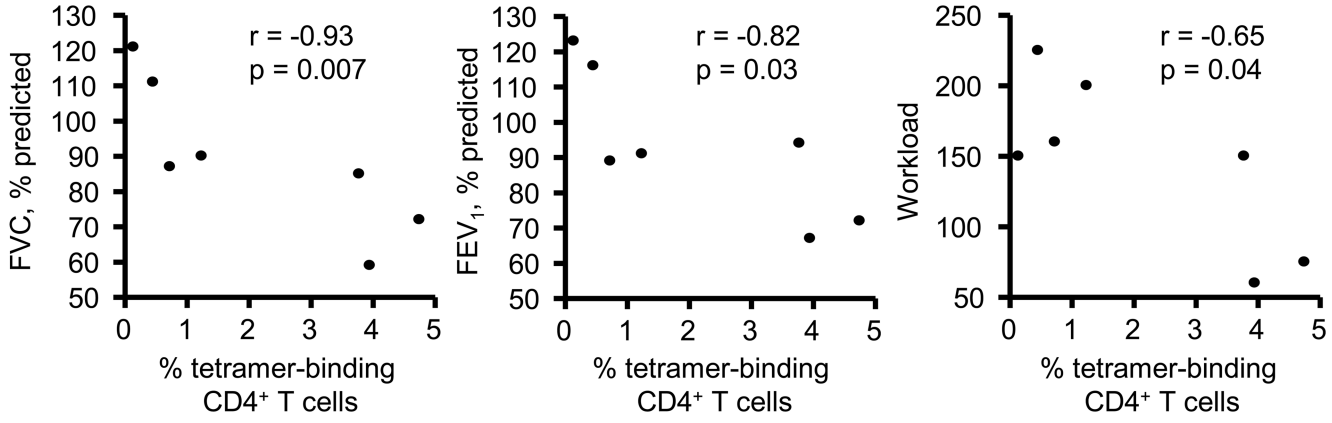

FIGURE 9.

Correlation between the percentage of HLA-DP2-mimotope-2/Be tetramer-binding $CD4^+$ T cells and parameters of lung function in 7 CBD patients. Lung function parameters included the percent predicted of the forced vital capacity (FVC) and the forced expiratory volume in 1 second (FEV_1) as well as workload as a measure of exercise capacity.